

## ORIGINAL RESEARCH ARTICLE

# Morris method with improved sampling strategy and Sobol' Variance-based method, as validation tool on Numerical Model of Richard's Equation

Sunny Goh\*

School of Ocean Engineering, University Malaysia Terengganu, Kuala Terengganu 21030, Terengganu, Malaysia. E-mail: sunny.goh@gmail.com

### ABSTRACT

Richard's equation was approximated by finite-difference numerical scheme to model water infiltration profile in variably unsaturated soil<sup>[1]</sup>. The published data of Philip's semi-analytical solution was used to validate the simulated results from the numerical scheme. A discrepancy was found between the simulated and the published semi-analytical results. Morris method as a global sensitivity tool was used as an alternative to local sensitivity analysis to assess the results discrepancy. Morris method with different sampling strategies were tested, of which Manhattan distance method has resulted a better sensitivity measures and also a better scan of input space than Euclidean method. Moreover, Morris method at  $p = 2$ ,  $r = 2$  and Manhattan distance sampling strategy, with only 2 extra simulation runs than local sensitivity analysis, was able to produce reliable sensitivity measures ( $\mu^*$ ,  $\sigma$ ). The sensitivity analysis results were cross-validated by Sobol' variance-based method with 150,000 simulation runs. The global sensitivity tool has identified three important parameters, of which spatial discretization size was the sole reason of the discrepancy observed. In addition, a high proportion of total output variance contributed by parameters  $\beta$  and  $\theta_s$  is suggesting a greater significant digits to reduce its input uncertainty range.

**Keywords:** Richard's Equation; Morris Method; Sobol's Variance-based Method; Euclidean Distance Sampling Strategy; Manhattan Distance Sampling Strategy; Global Sensitivity Analysis

### ARTICLE INFO

#### Article history:

Received 13 January 2021

Received in revised form 24 February 2021

Accepted 26 February 2021

Available online 6 March 2021

### COPYRIGHT

Copyright © 2021 Sunny Goh.

doi: 10.24294/jgc.v4i1.763

EnPress Publisher LLC. This work is licensed under the Creative Commons Attribution-NonCommercial 4.0 International License (CC BY-NC 4.0).

<https://creativecommons.org/licenses/by-nc/4.0/>

## 1. Introduction

Generally, there are two ways in testing sensitivity analysis. The commonly used method is to vary parameter value in certain percentage, i.e., 10, 20% or more<sup>[2-4]</sup>, and calculate the sensitivity coefficient. The second method is to calculate sensitivity indices based on uncertainty of parameters, which could be gathered from previous studies, for instance, in Fox *et al.*<sup>[5]</sup>. While the former provides an overall understanding of each parameter under a defined percentage boundary, the later allows propagation of parameter uncertainty into the corresponding uncertainty in model output.

Morris method provides qualitative sensitivity measures by ranking parameters, and those with the least important parameters could be fixed, without affecting model output<sup>[6]</sup>. Original Morris method utilizes mean ( $\mu$ ) and standard deviation ( $\sigma$ ) of elementary effect as screening procedure, while the improved Morris method by Campolongo *et al.* introduced absolute mean of elementary effect ( $\mu^*$ ) as a complementary to existing<sup>[7]</sup>. Also, the original Morris method generates a number of random trajectories, while Campolongo *et al.* introduce a

new sampling strategy using Euclidean distance method to identify a group of trajectories with the greatest spread<sup>[7]</sup>. They have shown that the new sampling strategy is able to provide a reliable approximation to total effect index ( $S_{Ti}$ ) at lower simulation runs. However, this sampling method is not widely used. Some researches continue to use original Morris sampling strategy, for instance, Drouet *et al.* on nitrous oxides emissions at farm level<sup>[8]</sup>, and Chu-Agor *et al.* on the vulnerability of coastal habitats to sea level rise<sup>[9]</sup>. Apart from the Euclidean distance method, Campolongo *et al.* suggested that an alternative method, i.e., Manhattan distance, should be investigated and compared to existing Euclidean distance method<sup>[7]</sup>. In this study, we compare these methods as one of the objectives.

Morris method is suitable for factor fixing but not for factor prioritization<sup>[10]</sup>, although effort has been made to improve this method into quantitative approach by increasing simulation runs<sup>[11]</sup>. In this study, we would like to focus on the advantage of improved Morris method by Campolongo *et al.* as a screening tool. It is commonly accepted in the literature that the 4 levels of input space and/or the 10 random trajectories are sufficient to produce a valuable results<sup>[10,11-15]</sup>. Some other researchers would prefer different combination of levels and trajectories, such as 5 levels, 120 trajectories in Drouet *et al.*<sup>[8]</sup>, and 10 levels, 100 trajectories in Moreau *et al.*<sup>[16]</sup>. In this study, we would like to determine the extent to which the levels and trajectories could be reduced, while maintaining its screening ability as an objective of our study. The motivation is obvious because the fewer the trajectory is, the fewer simulation runs would be required, which is a direct indication of lesser computational time. This approach is motivated by Saltelli and Annoni<sup>[17]</sup>:

“[...] non quantitative results can be obtained for screening purposes [...] but already two trajectories can be quite informative as they give a double estimate for the effect of each factor, and by difference of these, an idea of the deviation from linearity acquired.”

Quantitative method, for example, variance-based method, can be applied for both factor fix-

ing and factor prioritization, but high in computational cost. Variance-based method is a model free uncertainty analysis tool, and thus, it is used in various applications for sensitivity analysis, such as Kinetic Model for OH-initiated oxidation of DMS<sup>[13]</sup>, HYMOD model<sup>[18]</sup>, flood inundation model (HEC-RAS)<sup>[19]</sup>, dynamic responses of tomato to environment (TOMGRO)<sup>[20]</sup>, to improve process in mineral processing<sup>[21]</sup>, ecological model<sup>[22]</sup>, etc. The usage of variance-based method is to quantify the variance contribution of input parameters to the unconditional variance of model output. This tool is generally applied to determine first order index ( $S_i$ ) and total effect index ( $S_{Ti}$ ). In this study, variance-based method<sup>[7]</sup> is used as a tool to cross-validate the results from improved Morris method.

In general, sensitivity analysis can be used for various reasons<sup>[23]</sup>. In model development, it can be used for the purposes of model validation or accuracy, simplification, calibration, coping with poor or missing data, and even to identify important parameter for further studies<sup>[24]</sup>. The aim of this study is to utilize sensitivity analysis method as a validation tool on Richard's equation<sup>[25]</sup>, i.e., to validate simulation results with published Philip semi-analytical solution<sup>[26,27]</sup>. Also, it is used to study the effect of uncertainty input parameters on variance of simulation output.

According to Namin and Boroomand, Richard's equation numerical solution strategy is still a subject to research<sup>[28]</sup>. In validating the simulation results to experimental and/or semi-analytical results, sensitivity analysis is one of the important steps that should be carried out, in the least to identify input parameter(s) responsible for discrepancy between simulation and experimental and/or semi-analytical results. There are studies on Richard's equation which would benefit from sensitivity analysis study, e.g., Ma *et al.*<sup>[29]</sup> and Caviedes-Voullième *et al.*<sup>[30]</sup>. One of the simplest approaches to study sensitivity analysis is to assume  $\pm 20\%$  and  $\pm 40\%$  deviation from base value<sup>[8]</sup>.

## 2. Sensitivity analysis techniques

The relation of model output ( $Y$ ) and array of model input parameters ( $X$ ) can be written in the following form:

$$Y = f(X) = f(X_1, X_2, X_3, \dots, X_q) \quad (1)$$

Where,  $Y$  could be multiple outputs in terms space and time, or a single model output.

### 2.1 Improved Morris method

Morris proposed mean ( $\mu$ ) and standard deviation ( $\sigma$ ) of elementary effect ( $EE$ ) that is capable to distinguish input parameters into either: (a) negligible, (b) linear and additive, (c) non-linear, or (d) involved in interactions with other inputs. This method is different from the traditional sensitivity analysis, i.e., varying single input parameter one-at-a-time (OAT). Morris method has improved sensitivity analysis where each OAT of the input parameter of interest is generated at random value of other input parameters. The range of each parameter value is defined between 0 and 1. A technical scheme, Equation (2), to generate random trajectories is as following<sup>[6,10,15]</sup>:

$$B^* = \left\{ J_{k+1,k} x^* + \left( \frac{\Delta}{2} \right) [(2B - J_{k+1,k}) D^* + J_{k+1,k}] \right\} P^* \quad (2)$$

Where:  $B^*$  is the randomly generated trajectory in the form of matrix with dimension  $(k + 1) \times k$ , where  $k$  is the number of independent input parameters;  $\Delta$  is a value in  $[1/(p - 1), \dots, 1 - 1/(p - 1)]$  and  $p$  is the number of levels,  $J_{k+1,k}$  is  $(k + 1) \times k$  matrix of 1's;  $x^*$  is a randomly chosen base value;  $B$  is lower triangular matrix of 1's;  $D^*$  is  $k$ -dimensional diagonal matrix of which each element is either +1 or -1, by random generation; and  $P^*$  is  $k$ -by- $k$  random permutation matrix that each row with only one element equal to 1 and no column has more than one element that has 1.

Each trajectory consists of a random step for each input parameter that is either increase or decrease. For instance, Richard's equation has 10 input parameters to be tested, including time-step and spatial discretization size. Thus, there are 10 steps for each trajectory. Total simulation runs is based on  $N(k + 1)$ , which  $N$  refers to random trajectories generated. In this study, various values of  $N$  were tested. For example, for  $N = 10$ ,  $10(10 + 1) = 110$  simulation, runs would be required.

Campolongo *et al.* have proposed a new sampling strategy to compare geometric distance between pair of trajectories:

$$d_{ml} = \left\{ \sum_{i=1}^{k+1} \sum_{j=1}^{k+1} \sqrt{\sum_{z=1}^k [X_{z=1}^{(i)}(m) - X_{z=1}^{(j)}(l)]^2} \right\} \quad m \neq l \quad (3)$$

Where:  $d_{ml}$  is distance between a pair of trajectories  $m$  and  $l$ ;  $X_{z=1}^{(j)}(l)$  is  $z$ th coordinate of the  $j$ th point of the  $l$ th trajectory; and  $X_{z=1}^{(i)}(m)$  is  $z$ th coordinate of the  $i$ th point of the  $m$ th trajectory. They have shown that Equation (3), using Euclidean distance method, can be used to identify a small number of trajectories with the greatest spread. Thus, it reduced the number of trajectories needed to calculate absolute mean of elementary effect and its results shown to be a good approximation to total effect index ( $S_{Ti}$ ) as original Morris sampling method. Alternatively, they have also suggested Manhattan distance method should be tested, and the equation is shown as following:

$$d_{ml} = \left\{ \sum_{i=1}^{k+1} \sum_{j=1}^{k+1} \sum_{z=1}^k |X_{z=1}^{(i)}(m) - X_{z=1}^{(j)}(l)| \right\} \quad m \neq l \quad (4)$$

Where all terms are same, except the mathematical operation is simpler than the previous one.

The elementary effect ( $EE$ ), mean of elementary effect ( $\mu$ ), absolute mean of elementary effect ( $\mu^*$ ) and standard deviation of elementary effect ( $\sigma$ ) are as following<sup>[7,10,15]</sup>:

$$EE_i^j = \frac{y^j(X_1, X_2, \dots, X_i + \Delta_i, \dots, X_q) - y^j(X_1, X_2, \dots, X_i, \dots, X_q)}{\Delta_i} \quad (5)$$

$$\mu_i = \frac{1}{r} \sum_{j=1}^r EE_i^j \quad (6)$$

$$\mu_i^* = \frac{1}{r} \sum_{j=1}^r |EE_i^j| \quad (7)$$

$$\sigma_i^2 = \frac{1}{r-1} \sum_{j=1}^r (EE_i^j - \mu_i)^2 \quad (8)$$

Where:  $y^j(X_i)$  and  $y^j(X_i + \Delta_i)$  are simulation results before and after increment or decrement of  $\Delta$  value, i.e.,  $\Delta_i$  can either positive or negative value;  $r$  is referring to the total number of trajectories;  $EE_i^j$  is elementary effect of  $i$  input parameter at  $j$  trajectory; and  $\sigma_i$  is standard deviation of  $i$  input parameter.

### 2.2 Sobol' method

Sobol' method is based on decomposition of total unconditional variance,  $V(Y)$ , on Equation (1), into partial variances of increasing dimensionality (Sobol' 1990)<sup>[31]</sup>:

$$V(Y) = \sum_i^q V_i + \sum_i^q \sum_{j > i}^q V_{ij} + \dots + V_{12\dots q} \quad (9)$$

Where,  $V_i = V[E(Y|X_i)]$  is the sum of partial variances that include main effects of each input parameter,  $V_{ij} = V[E(Y|X_i, X_j)] - V_i - V_j$ , includes all the partial variances of two input parameters interaction, and the main effects. The  $E$  indicates expectation operator, and  $V$  is the variance operator.

The partial variances of Equation (9) divided by total unconditional variance to give:

$$\sum_i^q S_i + \sum_i^q \sum_{j > i}^q S_{ij} + \dots + S_{12\dots q} = 1 \quad (10)$$

Where,  $S_i = V_i/V(Y)$  is first order (or main effect) index;  $S_{ij} = V_{ij}/V(Y)$  is the second order index, i.e., also known as interaction effect between parameter  $i$  and  $j$ , and subsequently for other terms in Equation (10). The equation is exclusive for all input parameters that are independent, i.e., orthogonal from each other.

The ratio of partial variances (e.g.  $V_i$ ,  $V_{ij}$ , etc) to total variance ( $V(Y)$ ) indicates that all the sensitivity indices are scaled between 0 and 1 interval. When the summation of all first order indices gives unity, i.e.,  $\sum_i^q S_i = 1$ , the model is known as additive, i.e. without any interaction effect. Hence, the residual of  $1 - \sum_i^q S_i$  indicates interaction effects that could be a combination of second order or higher orders.

The total effect index ( $S_{T_i}$ ) for each input parameter is given by:

$$S_{T_i} = S_i + \sum_{i \neq j} S_{ij} + \sum_{i \neq j \neq l} S_{ijl} + \dots \quad (11)$$

As an example, if, total effect index would be given by:

$$S_{T_1} = S_1 + S_{12} + S_{13} + S_{123} \quad (12)$$

Where  $S_1$ ,  $S_{12}$ ,  $S_{13}$  and  $S_{123}$  are corresponding to first order index of input parameter 1, second order index of interaction effect between input parameters 1 and 2, second order index of parameters 1 and 3 and third order index of interaction effect between input parameters 1, 2 and 3. The total effect index for  $S_{T_2}$  and  $S_{T_3}$  can be decomposed with similar approach. Since  $S_{T_i}$  includes from first to higher order indices that relating to input parameter  $i$ ,  $S_{T_i} - S_i$  indicates only interaction effect that only account for second and higher order indices.  $S_i$  is used to indicate output variance that can be reduced if parameter  $X_i$  is fixed, and  $S_{T_i}$  represents output variance remains in model output, if  $X_i$  cannot be fixed<sup>[32]</sup>.

The first order sensitivity index and total effect index were estimated by quasi-Monte Carlo estimators<sup>[33]</sup>:

$$S_i = \frac{V(Y) - (1/2N) \sum_{m=1}^N (y_B^{(m)} - y_C^{(m)})^2}{V(Y)} \quad (13)$$

$$S_{T_i} = \frac{(1/2N) \sum_{m=1}^N (y_A^{(m)} - y_C^{(m)})^2}{V(Y)} \quad (14)$$

Where,  $y_A^{(m)}$ ,  $y_B^{(m)}$  and  $y_C^{(m)}$  are model outputs in Equation (13) and (14). Sobol' quasi-random sequences were used to generate two sets of data, i.e., matrix  $A$  and  $B$  corresponding to model outputs of  $y_A^{(m)}$  and  $y_B^{(m)}$ , and these dataset are confined between 0 and 1.  $V(Y)$  is:

$$(1/N) \sum_{m=1}^N (y_A^{(m)})^2 - f_o^2$$

Alternatives are Fourier Amplitude Sensitivity Test (FAST)<sup>[34,35]</sup> and Extended FAST<sup>[36]</sup>. In this study, we limit to Sobol' quasi-random sequence.

The  $f_o^2$  is given by:

$$(1/N) \sum_{m=1}^N (y_A^{(m)})^2.$$

The  $y_{C_i}^{(m)}$  model output was obtained by taking all the dimensions from matrix  $A$ , except  $i$  column, i.e., dimension is taken from matrix  $B$ . Richard's equation has 8 input parameters that must be tested, and thus, 8 dimensions were required for each matrix.

To solve Equations (13) and (14), we need two matrixes ( $A$  and  $B$ ), i.e.,  $2N$ , and  $k$  input parameters of  $N$  for each input parameter, i.e.,  $kN$ . In our study, we used  $N = 150000$  rows and  $k = 8$  columns, i.e., due to 8 input parameters. In total, we have to simulate for  $N(k + 2) = 15000(8 + 2) = 150000$  runs. The greater the  $N$  value is, the better the estimation of sensitivity indices will be, which stated by Nossent *et al.*<sup>[37]</sup>, where they have demonstrated that a  $N$  value of 12,000 for 26 input parameters is sufficient to obtain reliable estimation.

### 3. The governing equation of water flow in unsaturated soil, and its numerical solution

The governing equation for transient water flow in unsaturated soil, i.e., Richard's equation<sup>[25]</sup>, based on  $\theta_L$ -based form, is as following:

$$\frac{\partial \theta_L}{\partial t} = \frac{\partial}{\partial z} \left[ \left( K \frac{\partial \psi_m}{\partial \theta_L} \right) \frac{\partial \theta_L}{\partial z} - K \bar{k} \right] \quad (15)$$

Thus:  $\theta_L$  is volumetric water content ( $\text{m}^3 \text{m}^{-3}$ );  $t$  is time of simulation (s);  $z$  indicates vertical distance of simulation (m);  $K$  is hydraulic conductivity of the medium ( $\text{m s}^{-1}$ );  $\psi_m$  is matric pressure head (m);  $\vec{k}$  is vector unit with a value of positive one when it is vertically downwards.

Other forms of governing equation, i.e., -based and mixed-based, and their advantages and limitations are stated by Celia *et al.*<sup>[38]</sup>. We justify the selection of this equation due to its simplicity in relating volumetric water content in the storage term on the left side of the equation to the similar volumetric water content in the flux term on the right side of the equation. The first limitation, calculation degeneration in fully saturated media, was addressed using an approximate value for the  $\theta_L$  in few decimal points, and the approximate value would give the exact value of  $\theta_L$  when the value was rounded up. The second limitation, porous material discontinuities produce discontinuous volumetric water content profiles. It could cause problem in simulation, but we have not yet encounter such a difficulty, and the simulation model is thus so far successful in simulating the governing processes.

Equation (15) was approximated numerically and its algebra was implemented in FORTRAN 2008 using Simply FORTRAN Integrated Development Environment. The spatial discretization method used is termed as cell-centered finite difference. The finite difference algebra for Equation (15), i.e., used for sensitivity analysis in the current study is as following:

$$\frac{\theta_{L(k)^{n+1}} - \theta_{L(k)^n}}{\Delta t} = \frac{K_{k+\frac{1}{2}} \left( \frac{\partial \psi_m}{\partial \theta_L} \right)_{k+\frac{1}{2}}}{\Delta Z_k (0.5 \Delta Z_{k+1} + 0.5 \Delta Z_k)} (\theta_{L(k+1)^{n+1}} - \theta_{L(k)^{n+1}}) - \frac{K_{k-\frac{1}{2}} \left( \frac{\partial \psi_m}{\partial \theta_L} \right)_{k-\frac{1}{2}}}{\Delta Z_k (0.5 \Delta Z_k + 0.5 \Delta Z_{k-1})} (\theta_{L(k)^{n+1}} - \theta_{L(k-1)^{n+1}}) - \frac{K_{i,j,k+\frac{1}{2}} \vec{k} - K_{i,j,k-\frac{1}{2}} \vec{k}}{\Delta Z_k} \quad (16)$$

Where:  $k$  indicates a cell-centered number in  $z$ -direction in Cartesian coordinate system;  $\Delta t$ (s) is time-step size;  $\theta_{L(k)^n}$  ( $\text{m}^3 \text{m}^{-3}$ ) and  $\theta_{L(k)^{n+1}}$  ( $\text{m}^3 \text{m}^{-3}$ ) are indicating volumetric water content at old time level ( $n$ ) and new time level ( $n+1$ ), respectively;  $K_{k+1/2}$  ( $\text{m s}^{-1}$ ) is hydraulic conductivity at

the interface between cell  $k$  and  $k+1$ ;  $K_{k-1/2}$  ( $\text{m s}^{-1}$ ) is hydraulic conductivity at the interface between cell  $k-1$  and  $k$ ;  $(\partial \psi_m / \partial \theta_L)_{k+1/2}$  is partial derivative of  $\psi_m$  with respect to  $\theta_L$  at the interface between the cell  $k$  and  $k+1$ ;  $(\partial \psi_m / \partial \theta_L)_{k-1/2}$  is partial derivative of  $\psi_m$  with respect to  $\theta_L$  at the interface between the cell  $k-1$  and  $k$ ;  $\Delta Z_{k+1}$ (m),  $\Delta Z_k$ (m) and  $\Delta Z_{k-1}$ (m) are corresponding to the spatial sizes of spacing of cell  $k+1$ ,  $k$  and  $k-1$ .  $\theta_{L(k+1)^{n+1}}$  ( $\text{m}^3 \text{m}^{-3}$ ),  $\theta_{L(k)^{n+1}}$  ( $\text{m}^3 \text{m}^{-3}$ ) and  $\theta_{L(k-1)^{n+1}}$  ( $\text{m}^3 \text{m}^{-3}$ ) are the volumetric water contents at new time level of cell  $k+1$ ,  $k$  and  $k-1$ , respectively.

The numerical solution of Equation (16) was solved by a fully implicit cell-centered finite-difference scheme without any linearization. An iterative method was used to solve the mathematical algebra of Equation (16), i.e., Jacobi iteration<sup>[39]</sup>. For comparison purpose, modified Newton-Raphson method was also implemented<sup>[40]</sup>. A convergence factor criterion was used to indicate the condition for iteration termination process, i.e., absolute maximum difference  $|\theta_{L(k)^{n+1}} - \theta_{L(k)^n}|$  for every single cell.

#### 4. The constitutive functions of matric pressure head ( $\psi_m$ ) and hydraulic conductivity (K)

The constitutive functions implemented are from Haverkamp *et al.*<sup>[26]</sup>:

$$\psi_m = -10^{-2} \exp \left[ \frac{\alpha(\theta_s - \theta_r)}{\theta_L - \theta_r} - \alpha \right]^{\frac{1}{\beta}} \quad (17)$$

$$K = K_s \frac{A}{A + (-100\psi_m)^B} \quad (18)$$

Where:  $\alpha$ ,  $\beta$ ,  $A$  and  $B$  are fitting parameters;  $\theta_r$  ( $\text{m}^3 \text{m}^{-3}$ ) is residual volumetric water content;  $\theta_s$  ( $\text{m}^3 \text{m}^{-3}$ ) is saturated volumetric water content; and  $K_s$  ( $\text{m s}^{-1}$ ) is saturated hydraulic conductivity.

#### 5. Input parameters considered for local and global sensitivity analysis

Referring to Equations (17) and (18), there are basically 8 input parameters from Richard's equations. Out of those input parameters, 3 parameters are relating to hydraulic conductivity of soil medium, i.e., Equation (18), while the other 5 parameters are inputs for matric pressure head,

Equation (17). All the parameters are listed in **Table 1**. The uncertainty range for each parameter was developed based on either input parameter uncertainty or numerical input parameter uncertainty. For time-step size and spatial discretization size, they are termed as numerical input parameters because their influence on simulation output is depending on the implemented numerical solution, e.g. Caviedes-Voullième *et al.*<sup>[30]</sup>. Similar as Nossent *et al.*<sup>[37]</sup>, as we have no prior information on the parameters, the sensitivity analysis was carried out on uniform input parameters distribution. Some other researchers with similar assumption, e.g. Saltelli *et al.*<sup>[15]</sup> assumed uniform distribution for 103 parameters; Yang<sup>[18]</sup> assumed uniform distribution for 5 parameters, and Drouet *et al.*<sup>[8]</sup> assumed  $\pm 20\%$  and  $\pm 40\%$  from base value.

## 6. Numerical experiment and the default setting of input parameters of the flow problem

Water infiltration into Yolo light clay was used in the numerical experiment. The coefficients of the constitutive functions are tabulated in **Table 1**. Initial condition for the volumetric water content was  $0.2376 \text{ m}^3 \text{ m}^{-3}$ . Lower boundary was set permeable to inflow and outflow of water. Upper boundary was set at  $0.495 \text{ m}^3 \text{ m}^{-3}$ . Total simulation time was set to 600 s, and different time-step sizes were simulated to determine mass balance ratio (MBR) as given by Equation (19). This is required as part of a validation procedure since Celia *et al.*<sup>[38]</sup>. The formula of the equation is simply by taking the ratio of storage term over the flux term.

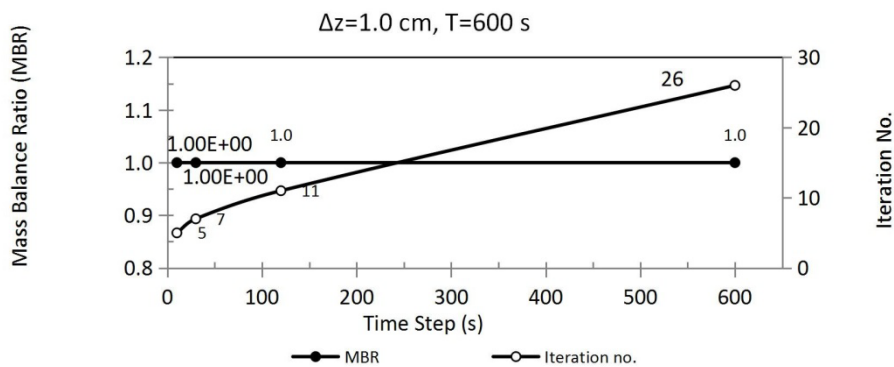


**Figure 1.** MBR and number of iteration at different time-step sizes, i.e., 10, 30, 120 and 600 s. Note that  $\Delta z$  is spatial spacing size, and T is the total simulation time.

**Table 1.** The coefficients value from Haverkamp *et al.* based on the constitutive Equations (17) and (18). These values were used as base case. Note that  $\theta_r$  is residual volumetric water content,  $\theta_s$  is saturated volumetric water content,  $K_s$  is saturated hydraulic conductivity, and  $\alpha$ ,  $\beta$ ,  $A$  and  $B$  are fitting coefficients.  $\theta_{L(initial)}$ ,  $\Delta z$  and  $\Delta t$  are initial spatial discretization size and time-step size, respectively.

<sup>a</sup>-Numerical input parameter uncertainty. All other parameters are based on Haverkamp constitutive equations.

Parameter	Base value	Distribution	Uncertainty analysis range
$\alpha$	739	Uniform	738.5 – 739.499
$\theta_r$	$0.124 \text{ m}^3 \text{ m}^{-3}$	Uniform	0.1235 – 0.124499
$\theta_s$	$0.495 \text{ m}^3 \text{ m}^{-3}$	Uniform	0.495 – 0.495499
$\beta$	4	Uniform	3.5 – 4.499
A	124.6	Uniform	124.55 – 124.6499
B	1.77	Uniform	1.765 – 1.77499
$K_s$	$4.428 \times 10^{-2} \text{ cm hr}^{-1}$	Uniform	$4.4275 \times 10^{-2}$ – $4.428499 \times 10^{-2}$
$\theta_{L(initial)}$	$0.2376 \text{ m}^3 \text{ m}^{-3}$	Uniform	0.23755 – 0.2376499
$\Delta z$	1 cm	Uniform	0.1 – 1 <sup>a</sup>
$\Delta t$	500 s	Uniform	10 – 500 <sup>a</sup>

Thus, we generalized the MBR equation in a more explicit form, but in a partial differential form, as following:

$$\text{MBR} = \sum_k^N \frac{(\frac{\partial \theta_L}{\partial t})_k}{\left\{ \frac{\partial}{\partial z} \left[ \left( K \frac{\partial \psi_m}{\partial \theta_L} \right) \frac{\partial \theta_L}{\partial z} - K \bar{k} \right] \right\}_k} \quad (19)$$

Where,  $k$  is the number of cell; and  $N$  is the total number of cell. The calculation of MBR was carried out for each time-step. A perfect simulation would give a MBR value of unity, and any increasing or decreasing in the value is indicating unwanted creation or loss of mass, respectively. Also, it should be noted that the MBR equation change according to the governing equation simulated.

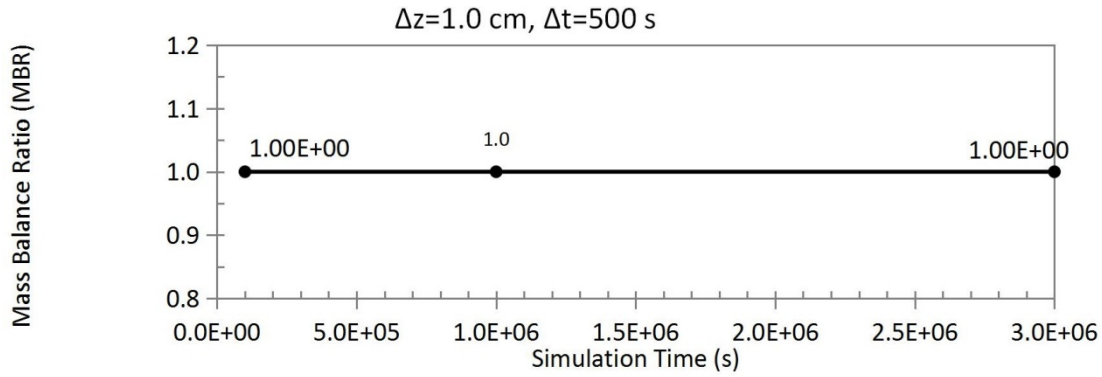


**Figure 2.** Mass balance ratio at different simulation times, i.e.,  $10^5$ ,  $10^6$  and  $3 \times 10^6$  s, at a time-step size of 500 s. Note that  $\Delta z$  is spatial spacing size, and  $\Delta t$  is time-step size.

**Figure 1** shows the MBR of the simulation is unity from 10 to 600 s of time-step size. Hence, in considering the increasing number of iteration due to increasing time-step value, the time-step was

taken as 500 s. By using the time-step, the simulation was preceded from 500 to  $3 \times 10^6$  s, and MBR in **Figure 2** does not show any sign of mass balance problem.

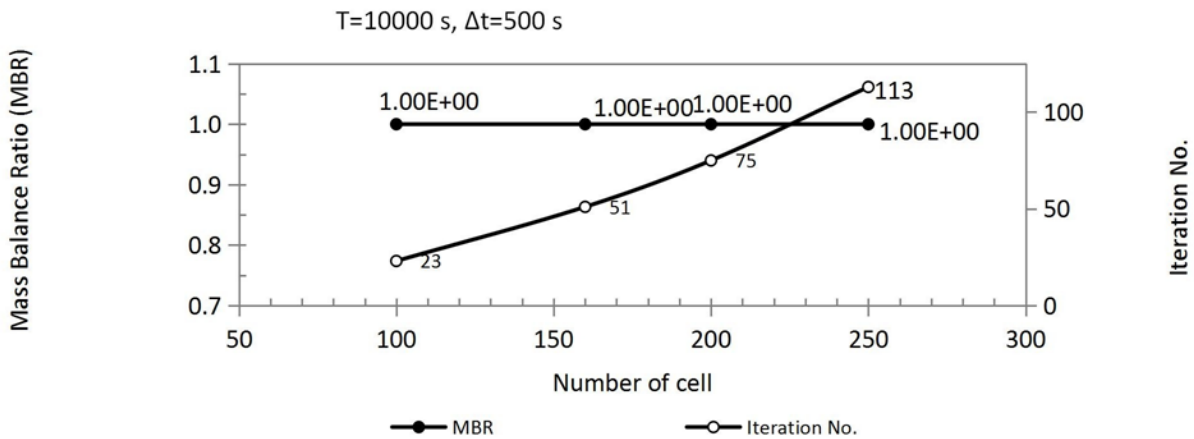


**Figure 3.** MBR and number of iteration at different cells number, i.e., 100, 160, 200 and 250 cells. The corresponding values of spatial spacing size ( $\Delta z$ ) are 2, 1.25, 1 and 0.8 cm. Note that  $\Delta t$  is time-step size, and T is the total simulation time.

The simulation medium was discretized into different spatial spacing sizes to investigate the simulation for any influence of number of cell on MBR and iteration number. The number of cell in the **Figure 3** is corresponding to spatial size of 2, 1.25, 1 and 0.8 cm. The result showed the spatial size does not have any influence on the MBR value, based on the range of simulation. However, the number of iteration increases at a greater rate than the increasing number of cell at high cell number. Thus, without causing excessive heavy load in computer processing time, the current work proceed with the number of cell use in the simulation at 200 cells, which is equivalent to 1 cm per cell, for a total depth of 200 cm.

The effect of convergence value (CV) on MBR and iteration number was investigated (see

**Figure 4**). At low convergence value,  $10^{-3} \text{ m}^3 \text{ m}^{-3}$ , it produced a MBR of 0.889. Despite it poses a desire property of having a low number of iteration. This is a serious mass problem, as 0.889 is equivalent to a mass loss of 11.1 % resulted by a single time-step before completing 105 s of simulation time. This could be explained by the fact that setting CV at  $10^{-3} \text{ m}^3 \text{ m}^{-3}$  is about accepting an error of 0.8 % and 0.2 % of and, respectively, for each cell of the simulation medium. Thus, at lower CV value would only result in unity MBR. Therefore, we stress the limit by setting MBR at  $10^{-12} \text{ m}^3 \text{ m}^{-3}$ , i.e., two orders of magnitude lower than  $10^{-10} \text{ m}^3 \text{ m}^{-3}$  that there is no significant change observed on the simulated value of volumetric water content, as shown in **Figure 5**. The effects of time-step and spatial spacing size on the

volumetric water content were not investigated here because those two parameters would be inves-

tigated in the sensitivity analysis as with other parameters.

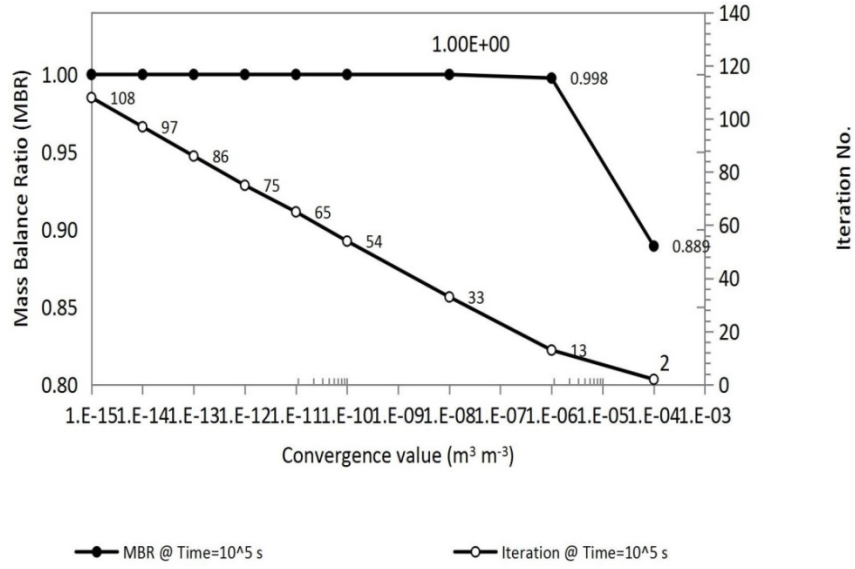


Figure 4. The influence of convergence value on MBR and iteration number.

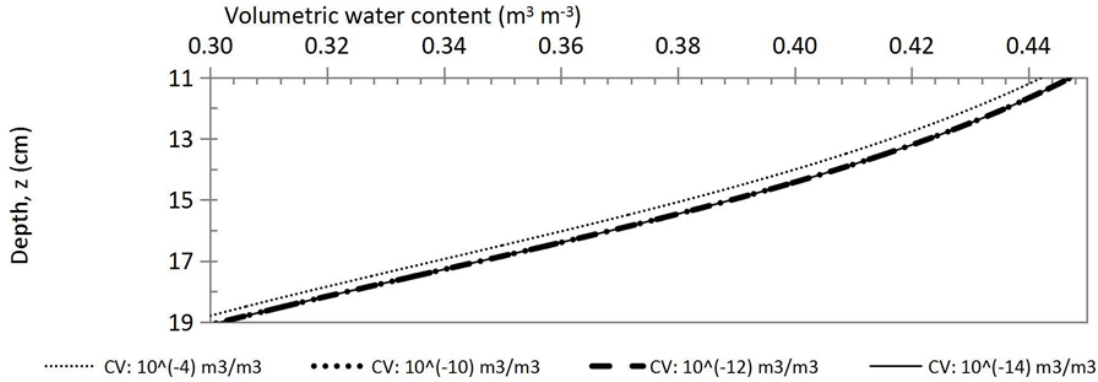


Figure 5. Simulation time of  $10^5$  s, at different convergence values (CV). Time-step, 500 s, and spatial spacing size, 1 cm.

The iteration methods of Jacobi and modified Newton-Raphson were compared. It was found that the minimum iteration number from the latter was equivalent to the iteration number from the former, when the relaxation factor of the latter was set to unity. Reducing the relaxation factor from unity would result in increasing iteration number. The numerical solution of Equation (15) did not exhibit convergent problem, thus, Jacobi iteration method is sufficient.

## 7. Statistical measures

In order to determine the goodness of fit between the data and the simulated results, some statistical equations were implemented. The equations are mean of residual error (M) and absolute residual errors (MA), respectively as following<sup>[41]</sup>:

$$M = \frac{1}{N} \sum_{k=1}^N (cal_k - obs_k) \quad (20)$$

$$MA = \frac{1}{N} \sum_{k=1}^N |cal_k - obs_k| \quad (21)$$

Where,  $cal_k$  is the simulated data at cell  $k$ ; and  $obs_k$  is the analytical solution at cell  $k$ .

## 8. Simulation results and its accuracy

Based on the conditions as stated in previous section, water infiltration into Yolo light clay was simulated up to  $3 \times 10^6$  s. Data on Philip's semi-analytical solution were collected from Haverkamp *et al.*<sup>[26]</sup>. Simulation results were compared with the data to verify the simulation (Figure 6). Before referring to any statistical measure, it was evident that the simulation results slightly under-predicted the infiltration flow of water front (Figure 7).

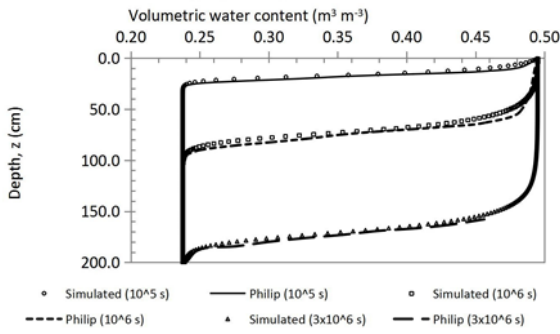


**Figure 6.** Simulation results and Philip's semi-analytical solution of water infiltration in Yolo light clay. Data for Philip's solution is from Haverkamp *et al.*

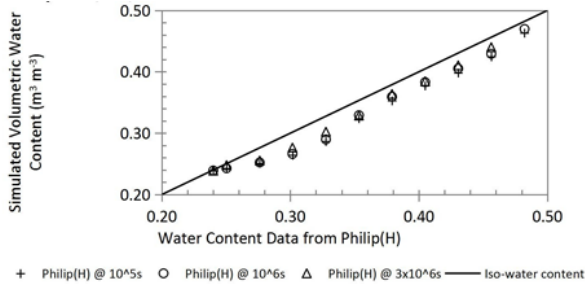


**Figure 7.** Overall comparisons of Philip's semi-analytical solution and simulated results. Philip(H) is referring to data from Haverkamp *et al.*

**Table 2.** Statistical calculations from Equations (20) and (21) at different simulation times. Note that M is mean of residual error, and MA is absolute residual errors

Error types	Simulation time (s)		
	10 <sup>5</sup>	10 <sup>6</sup>	3x10 <sup>6</sup>
M	-2.54x10 <sup>-2</sup>	-2.14x10 <sup>-2</sup>	-1.71x10 <sup>-2</sup>
MA	2.54x10 <sup>-2</sup>	2.14x10 <sup>-2</sup>	1.71x10 <sup>-2</sup>

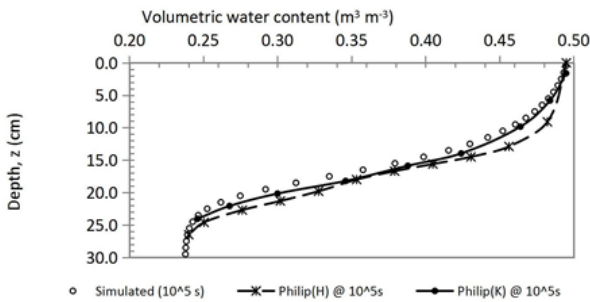


**Figure 8.** Comparison of simulated results with Philip's semi-analytical solution, Philip(H) and Philip(K) from Haverkamp *et al.*<sup>[26]</sup> and Kabala and Milly<sup>[27]</sup>, respectively.

Statistical equations, i.e. Equations (20) and (21), were used to justify goodness of fit between the simulated results and Philip's semi-analytical solution, as indicated by Philip(H) as in **Figure 7**, to further justify the reliability. The result is tabulated in **Table 2**. The mean of residual error (M) and absolute residual errors (MA) are having similar values, but the former value is in negative sign. This indicates that there is no single simulated data greater than the semi-analytical solution. Otherwise, the M value would be lesser

than its current value. These statistical results are agreed with the observation in **Figure 7**. In addition to this, the statistical results, in **Table 2**, also indicates that the developed computer simulation source code was indeed working properly. In order to further reinforce the previous claim, some data was extracted from Kabala and Milly<sup>[27]</sup>, as indicated by Philip(K) as in **Figure 8**, for further comparison. **Figure 8** shows that there is a small discrepancy between Philip(K) and Philip(H), but the former is relatively closer to the simulation results than the latter. At this point of observation, we are not able to determine which of the solutions provided from the literature is accurate. However, results from the figures and table clearly indicate that the simulated result is lesser than the Philip's semi-analytical solution. Therefore, sensitivity analysis was carried out to determine the sensitivity coefficient for all input parameters, and use the sensitivity analysis results to assess the model simulation based on the assumption that possibly the significant digits approximation, as in **Table 1**, could be contributing to the under prediction of the volumetric water content of the simulation.

As mentioned in previous section, we broadly termed the former as numerical input uncertainty and the latter as input parameter uncertainty. We justify the latter selection because the degree of uncertainty in the input parameters was not given, i.e., the published input data could be different from the exact value used by Haverkamp *et al.*<sup>[26]</sup> in simulating his results. Therefore, sensitivity analysis was carried out to determine the effect of the uncertainties influence on simulation outputs. Moreover, sensitivity analysis is one of the most important steps in evaluating the effect of input parameter on simulation results, and it is also used by other researchers for model validation<sup>[42-45]</sup>.

## 9. Local sensitivity analysis

Negligible sensitivity response could be resulted by too small perturbation size, and inaccuracy in sensitivity response could be due to too large perturbation size<sup>[46]</sup>. The input parameter values were subjected to a perturbation size between

-5% and 5% as suggested by Zheng and Bennett<sup>[41]</sup>. Some other perturbation sizes used by researchers, for example, 90 % in Vereecken *et al.*<sup>[2]</sup>, 20% in De Roo and Offermans<sup>[3]</sup>, and 10% in Davis *et al.*<sup>[4]</sup>. In considering the simulation time, we limit the sensitivity analysis to a simulation time of  $10^5$  s. The sensitivity analysis study was based on a single perturbation size of increment or decrement in each simulation.

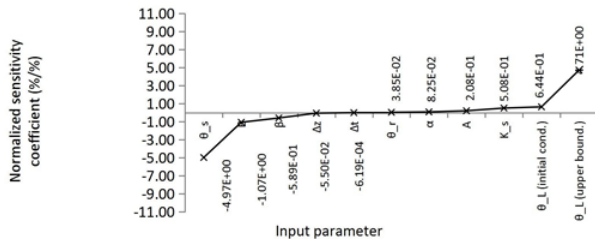


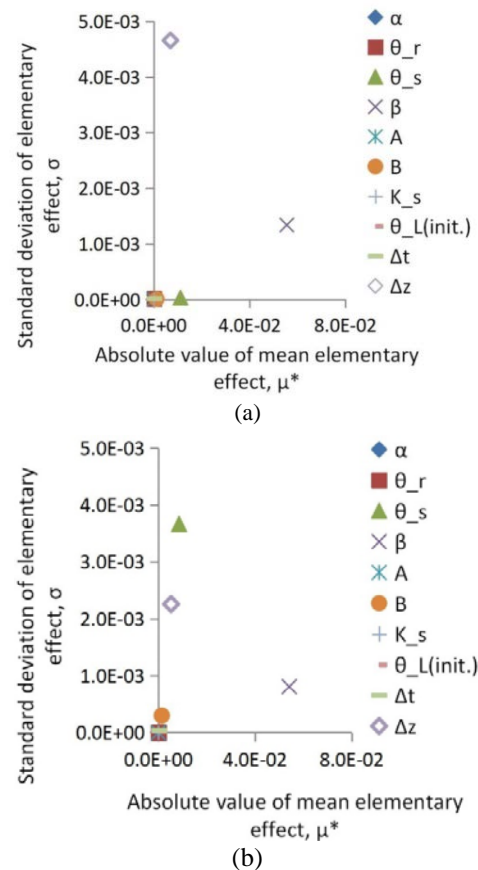
**Figure 9.** The rank of sensitivity coefficient. Note:  $\theta_s$  and  $\theta_r$  are saturated and residual volumetric water content;  $\Delta z$ , spatial spacing size;  $\Delta t$ , time-step size;  $K_s$ , saturated hydraulic conductivity;  $\theta_{L(initial\ cond.)}$ , clay medium initial value of volumetric water content;  $\theta_{L(upper\ bound.)}$ , upper boundary of volumetric water content; A, B,  $\beta$  and  $\alpha$  are fitting parameters from Haverkamp constitutive, as in Equations (17) and (18).

The normalized sensitivity coefficients are shown in **Figure 9**. Some other forms of presentation, for example, RMSE versus model parameters in Jhorar *et al.*<sup>[47]</sup>, relative sensitivity versus percentage change in parameter value in Vereecken *et al.*<sup>[2]</sup>, and TRMSE with parameter and time<sup>[48,49]</sup>. Generally, there are two groups sensitivity coefficient, i.e., positive and negative relations. In positive relation group, the boundary volumetric water content has the highest sensitivity coefficient. This is followed by initial volumetric water content and saturated hydraulic conductivity. The smallest sensitivity coefficient in the group is the residual volumetric water content. In negative relation group, saturated volumetric water content has the highest sensitivity coefficient, and this group ended with spatial spacing size and time-step size as the smallest sensitivity coefficient. The positive and negative relations were later couple with the range of uncertainty for each parameter to validate model simulation to semi-analytical solution. This procedure has been shown in Goh and Noborio<sup>[50]</sup>. Similarly, Cohen *et al.*<sup>[51]</sup> used local sensitivity analysis as part of its validation procedure on Richard's equation. Apart from the advantages of local sensitivity analysis, for example, at researcher convenient, its disad-

vantages have been proven by Saltelli and Annoni<sup>[17]</sup> through geometric proof, i.e., known as the curse of dimensionality.

## 10. Global sensitivity analysis

Based on Morris method, only the input parameters separated from the origin of relation  $\sigma$  versus  $\mu^*$  is considered important. From **Figure 10**, two groups of input parameter could be identified. Those important parameters were  $\beta$ , saturated volumetric water content ( $\theta_s$ ) and spatial discretization size ( $\Delta z$ ). The number of significantly important parameters was reduced from 10 to 3. Those parameters considered unimportant that they have limited influence on model output were:  $\alpha$ , residual volumetric water content ( $\theta_r$ ), initial volumetric water content of the medium ( $\theta_{L(initial)}$ ), from matric suction relation (Equation (17)); A, B and saturated hydraulic conductivity ( $K_s$ ) from hydraulic conductivity relation (Equation (18)); time-step size ( $\Delta t$ ) as numerical input parameter.



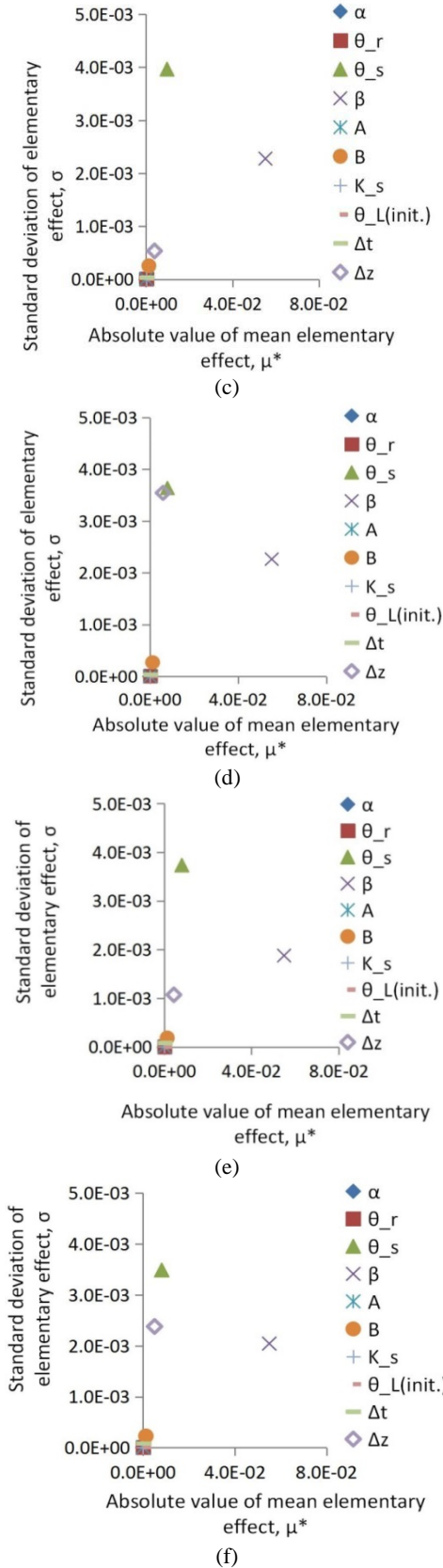


**Figure 10.** Global sensitivity analysis results from improved Morris method on Richard's equation at different levels ( $p$ ), trajectories ( $r$ ) and solved by either Euclidean or Manhattan method: (a)  $p = 2$ ,  $r = 2$ , Euclidean method; (b)  $p = 2$ ,  $r = 2$ , Manhattan method; (c)  $p = 4$ ,  $r = 4$ , Euclidean method; (d)  $p = 4$ ,  $r = 4$ , Manhattan method; (e)  $p = 4$ ,  $r = 10$ , Euclidean method; and (f)  $p = 4$ ,  $r = 10$ , Manhattan method.

The significant influence from parameter  $\Delta z$  was expected as the previous study on local sensitivity analysis has shown similar result<sup>[50]</sup>. However, the parameters  $\beta$  and  $\theta_s$  were unexpected. In parameter ranking, based on the values of  $\mu^*$ ,  $\beta$  was indeed the most important parameter, and then, followed by  $\theta_s$ ,  $\Delta z$ , and so on. It is widely accepted that the absolute mean value of elementary effect is to indicate the influence of parameter on model output<sup>[10,15]</sup>. Hence, a wide input range in **Table 1**, for parameters  $\beta$  and  $\theta_s$ , was the reason of high  $\mu^*$ . Goh and Noborio found that parameter with the high percentage of uncertainty and normalized sensitivity coefficient would result in large variation in model output<sup>[50]</sup>.

Parameters  $\beta$ ,  $\theta_s$  and  $\Delta z$  were found to have the highest standard deviation of elementary effect ( $\sigma$ ). The high value of the  $\sigma$  is an indication of parameter having non-linearity effect or involved in interactions with other factors<sup>[6,10,13]</sup>. In a fundamental level, a high value of  $\sigma$  is also suggesting that a large fluctuation of value or sign in the elementary effect ( $EE$ ). The other 7 parameters could be categorized as mainly linear and additive, as indicated by their low  $\sigma$  value.

In original Morris sampling strategy<sup>[6]</sup>, geometric distance between trajectories was not considered. This method is acceptable when a large number of random trajectories are generated, because all the input space of parameters would be fully explored. In search for cost effective sensitivity analysis tool to reduce computational time, the fewer trajectories would translate into lesser computational cost. Euclidean distance method as sampling strategy, as in Equation (3), was first coined by Campolongo *et al.*<sup>[7]</sup>. They have demonstrated that the improved sampling strategy could significantly reduce the number on **Figure 10(b)**,  $\Delta z$  in **Figures 10(d)** and **(f)**. In addition to this, **Figure 11** has shown Manhattan distance has a better sampling strategy as it exhibits lower variation in input space distribution as indicated by its lower standard deviation values than those of Euclidean distance sampling strategy.

By comparing Morris method between different levels ( $p = 2 - 4$ ), trajectories ( $r = 2 - 10$ ) and sampling strategies (Manhattan or Euclidean), we have found  $p = 2$ ,  $r = 2$  and Manhattan

distance sampling strategy was sufficient to provide reliable distinction between important and unimportant parameters. The computational experiment was carried out on an upper limit of  $p = 4$ ,  $r = 10$ , because it is greatly accepted that this limit would be sufficient to produce valuable results<sup>[12-14]</sup>. Moreover, these results would be cross-validated by Sobol' variance-based method.

f trajectories are needed, while maintaining a good approximation to total effect index. In addition to Euclidean distance method, there is also Manhattan distance method as stated in Campolongo *et al.*<sup>[7]</sup>, but not tested. In general, **Figures 10(a), (c) and (e)** have shown that at different levels ( $p$ ) and trajectories ( $r$ ), Euclidean distance has a comparable results as the Manhattan distance sampling strategy in **Figures 10(b), (d) and (f)**. However, a better estimation of  $\sigma$  was shown by Manhattan distance method on parameter  $\theta_s$ .

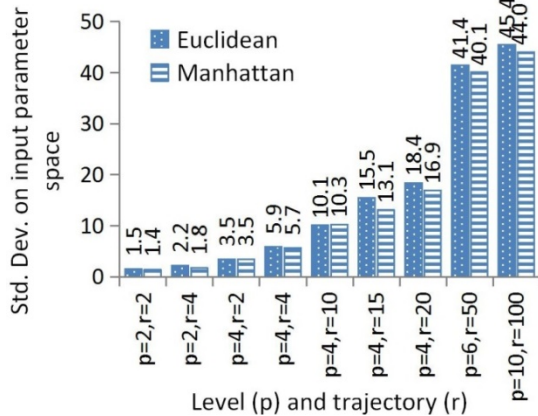


**Figure 11.** Standard deviation on input parameter space versus level ( $p$ ) and trajectory ( $r$ ).

An added advantage of  $p = 2$ ,  $r = 2$ , and Manhattan distance sampling strategy is that it only requires  $2 \text{ trajectories} \times (10 \text{ parameters} + 1) = 22$  simulation runs, while local sensitivity analysis with 10 parameters would require at least  $2 \times (10 \text{ parameters}) = 20$  runs, i.e., one run for each value of lower and upper range for each parameter. Irrespective of the number of parameters, the former is always only 2 runs greater than the latter. In addition, the parameter sensitivity measures of the former were estimated randomly at various input spaces of other parameters, while the latter was estimated by varying input space of parameter of interest and keeping other parameters constant. It is also important to note that the former is based on statistical theory, whereas the latter is

not. Therefore, it is compelling to practice Morris method of  $p = 2$ ,  $r = 2$ , and Manhattan distance sampling strategy with only 2 runs extra from Sobol' variance-based method was carried out to cross-validate the results from Morris method. All parameters were subjected to variance-based analysis, except spatial discretization size and time-step size, because their computational time would be too long to be executed efficiently. Nevertheless, the 8 parameters'  $\mu^*$  values from Morris method at  $p = 2$ ,  $r = 2$  (Manhattan distance sampling strategy) were compared to total effect index ( $S_{T_i}$ ) of Sobol' variance-based method, i.e., the results of 150,000 runs using quasi-Monte Carlo estimator (Equation (14)), referring to **Figure 12** local sensitivity analysis.

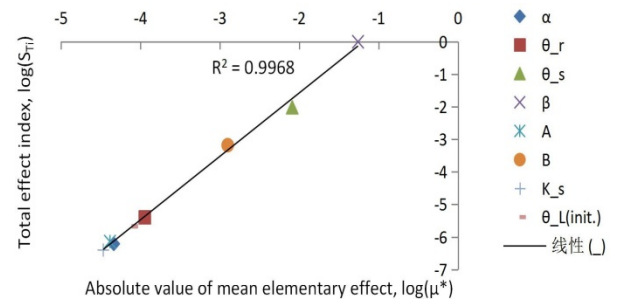


**Figure 12.** Total effect index ( $S_{T_i}$ ) versus absolute value of mean elementary effect ( $\mu^*$ ).

There were good agreements between those two for all 8 parameters. Similar effort in justifying the validity of results from Morris method by comparing  $\mu^*$  with  $S_{T_i}$  was showed by Campolongo *et al.*<sup>[7]</sup>. Thus, it indicates the absolute mean of elementary effect from Morris method of  $p = 2$ ,  $r = 2$  (Manhattan distance sampling strategy) was indeed correctly determined. In addition, the results of  $S_i$ , in **Table 3**, has shown similar trend as the  $S_{T_i}$ .

**Table 3.** First order sensitivity index ( $S_i$ ) and total effect index ( $S_{T_i}$ ) on input parameters. Note that  $\theta_r$  is residual volumetric water content,  $\theta_s$  is saturated volumetric water content,  $K_s$  is saturated hydraulic conductivity, and  $\alpha$ ,  $\beta$ ,  $A$  and  $B$  are fitting coefficients.  $\theta_{L(initial)}$ ,  $\Delta z$  and  $\Delta t$  are initial spatial discretization size and time-step size, respectively

Input parameters	Model outputs ( $\div 100$ )		
Total	0.0000	0.0001	0.0001
	0.0000	0.0004	0.0004
	0.9038	0.9631	0.0593
	98.9704	99.0293	0.0589
	0.0000	0.0001	0.0001
	0.0136	0.0663	0.0527
	0.0000	0.0000	0.0000
	0.0000	0.0002	0.0002
	99.887	100.0596	

The total sum of first order sensitivity index ( $\sum_i^q S_i$ ) was slightly less than one, which indicates the presence of interaction effect, i.e., second order and higher orders. The  $S_{T_i} - S_i$  indicates the presence of interaction effects between parameters, but it was found that each parameter has negligible contribution on model output variance, for instance, 0.06 % of output variance was contributed by  $\theta_s$  interactions with other parameters, which was among the highest.

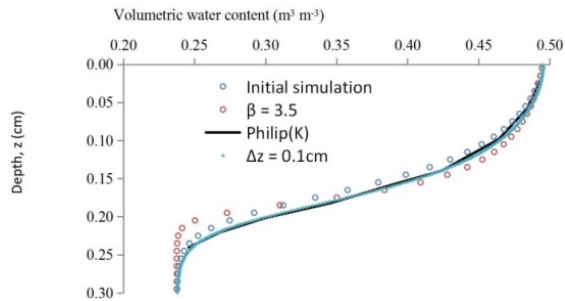


**Figure 13.** Water infiltration profile by numerical solution and semi-analytical solution. The validation was carried out with  $\beta$  at 3.5 and spatial discretization size at 0.1 cm. The initially simulated water profile is also included in the graph for comparison purpose. The total simulation time was  $10^5$  s.

In previous section, water infiltration was simulated using Richard's equation and was found to under predict the semi-analytical solution, referring to **Figures 6-8**. An overall summary of global sensitivity analysis has indicated that three important parameters, i.e.,  $\Delta z$ ,  $\beta$  and  $\theta_s$ , out of 10 parameters. This suggests the parameters have significant influence on model outputs. Based on the sensitivity analysis results, to increase the advancement of water infiltration profile is either to reduce single or a combination parameters among  $\Delta z$ ,  $\beta$  and  $\theta_s$ . The  $\theta_s$  value cannot be less than  $0.495 \text{ m}^3 \text{ m}^{-3}$ , because it would cause simulation failure, and hence, it was excluded. Single adjustment of  $\Delta z$  value was sufficient to result in good approximation of numerical solution to semi-analytical solution than the  $\beta$ . The validation results are showed in **Figure 13**. Therefore,  $\Delta z$  was the sole reason of the discrepancy between simulation result and semi-analytical solution.

## 11. Conclusions

Global sensitivity analysis tool of Morris method with extended sampling strategy, i.e., Euclidean distance method, by Campolongo *et al.*

was implemented and compared with Manhattan distance sampling strategy. They were tested on Richard's equation, which is commonly used to govern water flow in variably unsaturated soils. The absolute mean of elementary effect ( $\mu^*$ ) estimated by Morris method with Manhattan sampling strategy has comparable results to those with Euclidean distance method. However, the standard deviation of elementary effect ( $\sigma$ ) estimated through Manhattan method has proven better results than Euclidean method. Moreover, Manhattan method has a better scan of input space as indicated by lower standard deviation on input parameter space distribution than Euclidean method. Even at  $p = 2$ ,  $r = 2$  which only has 2 extra runs than the local sensitivity analysis, it was able to provide reliable estimation of sensitivity measures. The simulated results were cross-validated by sensitivity index of Sobol' variance-based method, of which  $\mu^*$  has shown consistent relation with total effect index ( $S_{T_i}$ ). The global sensitivity analysis also managed to identify three important parameters, of which the spatial discretization size ( $\Delta z$ ) was later found responsible for the discrepancy observed. This analysis suggests a better spatial numerical scheme should be implemented, or the numerical scheme would have to use a smaller  $\Delta z$  for accurate simulation. In addition, a great proportion of total output variance was contributed by  $\beta$  and  $\theta_s$ , which suggests a higher parameter significant digits published with lower input value uncertainty would reduce their variance contribution on the total output.

## Conflict of interest

No conflict of interest was reported by the author.

## References

1. Caviedes-Voullième D, Garcí'a-Navarro P, Murillo J. Verification, conservation, stability and efficiency of a finite volume method for the 1D Richards equation. *Journal of Hydrology* 2013; 480: 69–84.
2. Vereecken H, Maes J, Feyen J. Estimating unsaturated hydraulic conductivity from easily measured soil properties. *Soil Science* 1990; 149(1): 1–12.
3. De Roo APJ, Offermans RJE. LISEM: a physically-based hydrological and soil erosion model for basin-scale water and sediment management. In:

- Simonovic SP, Kundzewicz ZW, Rosbjerg D, *et al.* (editors). *Modelling and Management of Sustainable Basin-scale Water Resource Systems* (Proceedings of a Boulder Symposium). Oxfordshire: IAHS Publication; 1995. p. 399–407.
4. Davis A, Kamp S, Fennemore G, *et al.* Environmental policy analysis, peer reviewed: A risk-based approach to soil remediation modeling. *Environmental Science & Technology* 1997; 31(11): 520A–525A. doi: 10.1021/es9725662.
  5. Fox GA, Muñoz-Carpena R, Sabbagh GJ. Influence of flow concentration on parameter importance and prediction uncertainty of pesticide trapping by vegetative filter strips. *Journal of Hydrology* 2010; 384(1-2): 164–173. doi: 10.1016/j.jhydrol.2010.01.020.
  6. Morris MD. Factorial sampling plans for preliminary computational experiments. *Technometrics* 1991; 33(2): 161–174. doi: 10.2307/1269043.
  7. Campolongo F, Cariboni J, Saltelli A. An effective screening design for sensitivity analysis of large models. *Environmental Modelling & Software* 2007; 22(10): 1509–1518. doi: 10.1016/j.envsoft.2006.10.004.
  8. Drouet JL, Capian N, Fiorelli JL, *et al.* Sensitivity analysis for models of greenhouse gas emissions at farm level. Case study of N<sub>2</sub>O emissions simulated by the CERES-EGC model. *Environmental Pollution* 2011; 159(11): 3156–3161. doi: 10.1016/j.envpol.2011.01.019.
  9. Chu-Agor ML, Muñoz-Carpena R, Kiker G, *et al.* Exploring vulnerability of coastal habitats to sea level rise through global sensitivity and uncertainty analyses. *Environmental Modelling & Software* 2011; 26(5): 593–604. doi: 10.1016/j.envsoft.2010.12.003.
  10. Saltelli A, Ratto M, Andres T, *et al.* Elementary effects method. In: *Global Sensitivity Analysis. The Primer*. New York: John Wiley & Sons, Inc.; 2008. p. 109–154.
  11. Campolongo F, Saltelli A, Cariboni J. From screening to quantitative sensitivity analysis. A unified approach. *Computer Physics Communications* 2011; 182(4): 978–988. doi: 10.1016/j.cpc.2010.12.039.
  12. Campolongo F, Saltelli A. Sensitivity analysis of an environmental model: An application of different analysis methods. *Reliability Engineering & System Safety* 1997; 57(1): 49–69. doi: http://dx.doi.org/10.1016/S0951-8320(97)00021-5.
  13. Campolongo F, Tarantola S, Saltelli A. Tackling quantitatively large dimensionality problems. *Computer Physics Communications* 1999; 117(1-2): 75–85. doi: 10.1016/S0010-4655(98)00165-9.
  14. Saltelli A, Chan K, Scott EM (editors). *Sensitivity analysis. Wiley series in probability and statistics*. New York: John Wiley & Sons, Inc.; 2000. p. 494.
  15. Saltelli A, Tarantola S, Campolongo F, *et al.* The Screening Exercise. In: McCulloch A (editor). *Sensitivity Analysis in Practice: A Guide to Assessing Scientific Models*. New York: John Wiley & Sons, Inc.; 2004. p. 91–108.
  16. Moreau P, Viaud V, Parnaudeau V, *et al.* An approach for global sensitivity analysis of a complex environmental model to spatial inputs and parameters: A case study of an agro-hydrological model. *Environmental Modelling & Software* 2013; 47: 74–87. doi: http://dx.doi.org/10.1016/j.envsoft.2013.04.006.
  17. Saltelli A, Annoni P. How to avoid a perfunctory sensitivity analysis. *Environmental Modelling & Software* 2010; 25(12): 1508–1517. doi: 10.1016/j.envsoft.2010.04.012.
  18. Yang J. Convergence and uncertainty analyses in Monte-Carlo based sensitivity analysis. *Environmental Modelling & Software* 2011; 26(4): 444–457. doi: http://dx.doi.org/10.1016/j.envsoft.2010.10.007.
  19. Pappenberger F, Beven KJ, Ratto M, *et al.* Multi-method global sensitivity analysis of flood inundation models. *Advances in Water Resources* 2008; 31(1): 1–14. doi: http://dx.doi.org/10.1016/j.advwatres.2007.04.009.
  20. Vazquez-Cruz MA, Guzman-Cruz R, Lopez-Cruz IL, *et al.* Global sensitivity analysis by means of EFAST and Sobol' methods and calibration of reduced state-variable TOMGRO model using genetic algorithms. *Computers and Electronics in Agriculture* 2014; 100, 1–12. doi: 10.1016/j.compag.2013.10.006.
  21. Sepúlveda FD, Cisternas LA, Gálvez ED. The use of global sensitivity analysis for improving processes: Applications to mineral processing. *Computers & Chemical Engineering* 2014; 66: 221–232. doi: 10.1016/j.compchemeng.2014.01.008.
  22. Lagerwall G, Kiker G, Muñoz-Carpena R, *et al.* Global uncertainty and sensitivity analysis of a spatially distributed ecological model. *Ecological Modelling* 2014; 275: 22–30. doi: http://dx.doi.org/10.1016/j.ecolmodel.2013.12.010.
  23. Saltelli A, Ratto M, Andres T, *et al.* Variance-Based Methods. In: *Global Sensitivity Analysis. The Primer*. New York: John Wiley & Sons, Inc.; 2008. p. 155–182.
  24. Pannell DJ. Sensitivity analysis of normative economic models: theoretical framework and practical strategies. *Agricultural Economics* 1997; 16(2): 139–152. doi: 10.1016/S0169-5150(96)01217-0.
  25. Richards LA. Capillary Conduction of Liquids through Porous Mediums. *Journal of Applied Physics* 1931; 1(5): 318–333. doi: 10.1063/1.1745010.
  26. Haverkamp R, Vauclin M, Touma J, *et al.* A comparison of numerical simulation models for one-dimensional infiltration. *Soil Science Society of America Journal* 1977; 41(2): 285–294. doi: 10.2136/sssaj1977.03615995004100020024x.
  27. Kabala ZJ, Milly PCD. Sensitivity analysis of flow in unsaturated heterogeneous porous media: Theory, numerical model, and its verification. *Water Resources Research* 1990; 26(4): 593–610. doi: 10.1029/WR026i004p00593.
  28. Namin MM, Boroomand MR. A time splitting algorithm for numerical solution of Richard's equation. *Journal of Hydrology* 2012; 444-445: 10–21.

- doi: <http://dx.doi.org/10.1016/j.jhydrol.2012.03.029>.
29. Ma Y, Feng S, Su D, *et al.* Modeling water infiltration in a large layered soil column with a modified Green-Ampt model and HYDRUS-1D. *Computers and Electronics in Agriculture* 2010; 71, Supplement 1: S40–S47. doi: <http://dx.doi.org/10.1016/j.compag.2009.07.006>.
  30. Cavedes-Voullième D, Garcí'a-Navarro P, Murillo J. Verification, conservation, stability and efficiency of a finite volume method for the 1D Richards equation. *Journal of Hydrology* 2013; 480: 69–84.
  31. Sobol IM. Sensitivity estimates for nonlinear mathematical models. *Matematicheskoe Modelirovanie* 1990; 2(1): 112–118.
  32. Tarantola S, Giglioli N, Jesinghaus J, *et al.* Can global sensitivity analysis steer the implementation of models for environmental assessments and decision-making? *Stochastic Environmental Research and Risk Assessment* 2002; 16(1): 63–76. doi: 10.1007/s00477-001-0085-x.
  33. Saltelli A, Annoni P, Azzini I, *et al.* Variance based sensitivity analysis of model output. Design and estimator for the total sensitivity index. *Computer Physics Communications* 2010; 181(2): 259–270. doi: <http://dx.doi.org/10.1016/j.cpc.2009.09.018>.
  34. Cukier RI, Fortuin CM, Shuler KE, *et al.* Study of the sensitivity of coupled reaction systems to uncertainties in rate coefficients. I Theory. *The Journal of Chemical Physics* 1973; 59(8): 3873–3878. doi: <http://dx.doi.org/10.1063/1.1680571>.
  35. Schaibly JH, Shuler KE. Study of the sensitivity of coupled reaction systems to uncertainties in rate coefficients. II Applications. *The Journal of Chemical Physics* 1973; 59(8): 3879–3888. doi: <http://dx.doi.org/10.1063/1.1680572>.
  36. Saltelli A, Tarantola S, Chan KPS. *Technometrics*, 1999, 41(1):39-56. A quantitative model-independent method for global sensitivity analysis of model output. *Technometrics* 1999; 41(1): 39–56. doi: 10.1080/00401706.1999.10485594.
  37. Nossent J, Elsen P, Bauwens W. Sobol' sensitivity analysis of a complex environmental model. *Environmental Modelling & Software* 2011; 26(12): 1515–1525. doi: <http://dx.doi.org/10.1016/j.envsoft.2011.08.010>.
  38. Celia MA, Bouloutas ET, Zarba RL. A general mass-conservative numerical solution for the unsaturated flow equation. *Water Resources Research* 1990; 26(7): 1483–1496. doi:10.1029/WR026i007p01483.
  39. Tu J, Yeoh GH, Liu C. *Computational fluid dynamics: A practical approach*. 2<sup>nd</sup> ed. Oxford, Walton: Butterworth-Heinemann; 2007.
  40. Istok J. Step 4: Solve System of Equations. In: *Groundwater Modeling by the Finite Element Method*. Washington, DC: American Geophysical Union; 2013. p. 171–225.
  41. Zheng C, Bennett GD. *Applied contaminant transport modeling*. 2<sup>nd</sup> ed. New York: John Wiley & Sons, Inc.; 2002.
  42. Stange F, Butterbach-Bahl K, Papen H, *et al.* A process-oriented model of N<sub>2</sub>O and NO emissions from forest soils: 2. Sensitivity analysis and validation. *Journal of Geophysical Research: Atmospheres* 2000; 105(D4): 4385–4398. doi: 10.1029/1999jd900948.
  43. Nathan R, Safriel UN, Noy-Meir I. Field validation and sensitivity analysis of a mechanistic model for tree seed dispersal by wind. *Ecology* 2001; 82(2): 374–388. doi: 10.1890/0012-9658(2001)082[0374:fvasao]2.0.co;2.
  44. Min CH, He YL, Liu XL, *et al.* Parameter sensitivity examination and discussion of PEM fuel cell simulation model validation: Part II: Results of sensitivity analysis and validation of the model. *Journal of Power Sources* 2006; 160(1): 374–385. doi: 10.1016/j.jpowsour.2006.01.080.
  45. Gosling SN, Arnell NW. Simulating current global river runoff with a global hydrological model: model revisions, validation, and sensitivity analysis. *Hydrological Processes* 2011; 25(7): 1129–1145. doi: 10.1002/hyp.7727.
  46. Poeter EP, Hill MC. *Documentation of UCODE: A computer code for universal inverse modeling*. Denver: DIANE Publishing; 1998.
  47. Jhorar RK, Bastiaanssen WGM, Feddes RA, *et al.* Inversely estimating soil hydraulic functions using evapotranspiration fluxes. *Journal of Hydrology* 2002; 258(1-4): 198–213. doi: [http://dx.doi.org/10.1016/S0022-1694\(01\)00564-9](http://dx.doi.org/10.1016/S0022-1694(01)00564-9).
  48. Tang Y, Reed P, Wagener T, *et al.* Comparing sensitivity analysis methods to advance lumped watershed model identification and evaluation. *Hydrology and Earth System Sciences* 2007; 3(6): 793–817. doi: 10.5194/hess-11-793-2007.
  49. Wagener T, Werkhoven KV, Reed P, *et al.* Multi-objective sensitivity analysis to understand the information content in streamflow observations for distributed watershed modeling. *Water Resources Research* 2009; 45(2). doi: 10.1029/2008WR007347.
  50. Goh EG, Noborio K. Sensitivity analysis on the infiltration of water into unsaturated soil. *Proceedings of Soil Moisture Workshop, Hiroshima University Tokyo Office in Campus Innovation Center*; 2013. p. 66–68.
  51. Cohen D, Person M, Daannen R, *et al.* Groundwater-supported evapotranspiration within glaciated watersheds under conditions of climate change. *Journal of Hydrology* 2006; 320(3-4): 484–500. doi: <http://dx.doi.org/10.1016/j.jhydrol.2005.07.051>.